



FR 95 00527

OMN

D

LAPP-EXP-94.18

5 October 1994

HIGH PRECISION MEASUREMENTS OF THE LUMINOSITY AT LEP

B. Pietrzyk

Laboratoire de Physique des Particules LAPP. IN2P3-CNRS.

F-74941 Annecy-le-Vieux, France

Abstract

The art of the luminosity measurements at LEP is presented. First generation LEP detectors have measured the absolute luminosity with the precision of 0.3-0.5%. The most precise present detectors have reached the 0.07% precision and the 0.05% is not excluded in future. Center-of-mass energy dependent relative precision of the luminosity detectors and the use of the theoretical cross-section in the LEP experiments are also discussed.

Invited talk at the "Radiative Corrections: Status and Outlook" Conference
Gatlinburg, TN, USA, June 27 - July 1, 1994

1

VOL 26 No 22

1. Introduction

The Z line shape is described by three parameters: M_Z , Γ_Z and σ_0 . The luminosity normalizes the line shape cross-section and thus it influences directly the precision of the σ_0 measurement. The relative luminosity error $\frac{\delta\mathcal{L}}{\mathcal{L}} = 10^{-3}$ changes the σ_0 by 42 pb and N_ν by 0.0075. However, only the center-of-mass energy dependent luminosity relative error contributes to the precision of M_Z and Γ_Z measurements.

For any process the number of events counted in the detector is equal to the cross-section for this process multiplied by the luminosity:

$$N = \sigma\mathcal{L}$$

So in order to measure the luminosity we need to count events for a process in which the cross-section is known:

$$\mathcal{L} = \frac{N}{\sigma_{known}}$$

Of course, in both cases, the efficiency of the detector has to be taken into account.

At LEP the "known" process is e^+e^- scattering at small angles. The 99% or more of this cross-section is described by the t-channel photon exchange. This process can be calculated in QED with, in principle, infinite precision. Practical problems to achieve this infinite precision are described in the talks of S. Jadach and E. Kuraev at this conference. The photon(t-channel) and Z (s-channel) interference is responsible for the rest of the cross-section; its relative contribution is decreasing with decreasing scattering angle.

The precision of the luminosity measurements at PEP and PETRA was 2-3%, at LEP it is now better than 10^{-3} . This talk will describe how this has been obtained.

There have been two generations of detectors at LEP. A first generation has reached the precision of 0.3-0.5% and the Bhabha counting rate in these detectors was similar to the Z counting rate. A second generation of detectors started to be introduced from September 1992. Their precision is 0.07-0.2% and their counting rate is up to 3 times the Z counting rate.

The Bhabha cross-section is decreasing very fast with increasing scattering angle

$$\frac{d\sigma}{d\Theta} \sim \frac{1}{\Theta^3}$$

The integrated cross-section depends on the minimum and maximum scattering angle

$$\sigma \sim \left(\frac{1}{\Theta_{min}^2} - \frac{1}{\Theta_{max}^2} \right) \approx \frac{1}{\Theta_{min}^2}$$

Thus the largest component of the experimental luminosity error is twice the relative error of the minimum scattering angle measurement

$$\frac{\delta\mathcal{L}}{\mathcal{L}} \approx \frac{2\delta\Theta_{min}}{\Theta_{min}} \approx \frac{2\delta R_{min}}{R_{min}}$$

The second half of the formula shows that the relative precision of the minimum scattering angle measurement is equal to the relative precision of the minimum detector radius measurement. Thus for R_{min} of 10 cm we need a precision of at least $50\mu\text{m}$ to obtain luminosity precision of 10^{-3} .

2. First generation LEP luminosity detectors and the experimental methods

The basic parameters of the first generation LEP luminosity detectors are presented in Table 1. Their minimum radii were limited by the beam pipe diameter which was 17 cm for ALEPH, DELPHI and OPAL and 12 cm for L3.

	distance (m)	R_{min} (cm)	R_{max} (cm)	Θ_{min} (mrad)	Θ_{max} (mrad)	technology
ALEPH LCAL	2.7	10	52	45	190	lead+prop. wire ch.
DELPHI SAT	2.5	10	40	43	135	lead+sc. fibers
L3 BGO	2.8	6.8	19	25	70	BGO
OPAL FD	2.4	11.5	29	48	120	lead+scintillator

Table 1: Basic parameters of the first generation detectors at LEP.

A high energy electron or photon entering an absorber produces an electromagnetic cascade called also shower of pair production and bremsstrahlung. Typical "absorber" material lead is used by ALEPH, DELPHI and OPAL. In lead the shower is produced but no information can be read out. Therefore these detectors are divided into lead slices (planes) sandwiched with proportional chambers (ALEPH LCAL¹), scintillating fibers (DELPHI SAT²) or scintillator (OPAL FD³). Distinctively L3 is using BGO⁴ as both absorber and reading medium.

Detectors are divided into "cells", the smallest part of the detector which can be read out in each plane. In LCAL and SAT they have dimensions of about 3×3 cm, in BGO of about 1.5×2 cm. FD has larger cells of about 15×4.5 cm but in fact the acceptance is defined by 1 cm tubes placed in a region of maximum shower development.

A shower produced in a detector gives rise to an electronic signal in few cells in each plane. A collection of adjacent cells forms a cluster. An average position of cells weighted with their deposited energy gives the cluster coordinates. A typical Bhabha event containing two clusters on the opposite sides of the interaction point is shown in Fig. 1. This is a way a detector sees Bhabha scattering. One or more radiative photons can create additional clusters. If an angle between particles is too

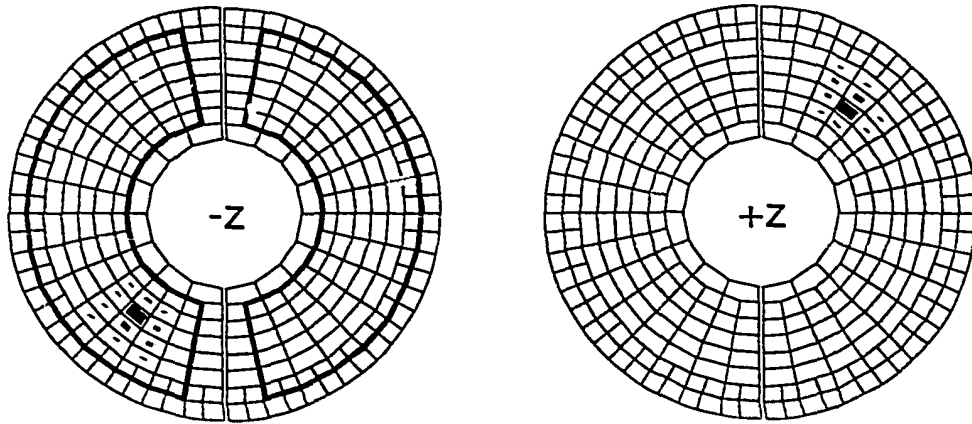


Figure 1: Geometrical acceptance and a cluster on each side in the L3 BGO detector.

small their clusters merge. Detector cannot distinguish between an electron and a photon (with one exception described later). The final state radiation photons emitted typically at small angle with respect to an electron or positron are integrated with them by the detector. Only the highest energy cluster on each side is accepted by the selection criteria.

Fig. 1 shows a typical geometrical acceptance of the LEP luminosity detectors. A solid line shows the "narrow" acceptance on one side, while the whole detector makes the "wide" acceptance on the other side. The "narrow-wide" and "wide-narrow" acceptance is applied to each event or alternating from event to event. Note also an insensitive region in ϕ , typical for the first generation LEP detectors. This insensitive region is there due to mechanical constraints related to the necessity of mounting two halves of the detector around the beam pipe.

The asymmetric acceptance is needed to reduce the dependence of the measured cross-section on the interaction point displacement. This dependence is canceled in the first order (linear dependence) if the difference in radius of the "wide" and "narrow" acceptance is larger than twice the vertical Δx , and horizontal Δy beam displacements:

$$\delta R > \max(2\Delta x, 2\Delta y, R \frac{2\Delta z}{Z})$$

Similar criteria have been derived for the displacement Δz along the beam direction in the formula above. If these criteria are fulfilled then only the second order (quadratic) errors contribute.

The asymmetric acceptance is applied differently by different experiments. ALEPH is alternating the "narrow" and "wide" acceptance, left, right, event by event. OPAL selects events by "wide" acceptance, then applies "narrow" cuts to $\frac{\Theta_L + \Theta_R}{2}$, where $\Theta_{L,R}$ are angles measured on two sides. For the second generation OPAL detector also \mathcal{L}_L and \mathcal{L}_R are measured* and corrected for by the vertex position fill by fill, then the mean $\mathcal{L} = \frac{\mathcal{L}_L + \mathcal{L}_R}{2}$ is the measured luminosity. L3 measures the Narrow-Wide and Wide-Narrow acceptance for each event and the measured luminosity is $\mathcal{L} = \frac{\mathcal{L}_{NW} + \mathcal{L}_{WN}}{2}$. DELPHI has a tungsten mask (which replaced the lead one) to define acceptance on one side, so the "narrow" and "wide" acceptance cannot alternate from side to side. However, since the acceptance is asymmetric and not alternating, the first order errors are canceled for Δx and Δy shifts; for Δz displacements corrections are applied fill by fill.

Another important experimental cut is the cut on the energy of the highest energy cluster on each side. The highest energy cluster distribution on one side against the one on the other side is shown on the Fig. 2. The data are shown as points. We clearly see events with no or small photon radiation (Born approximation), events where only one energetic photon has been emitted and only energy on one side has been lost ($O(\alpha)$ correction) and events where energy has been lost on both sides (higher order corrections). The solid line shows the software energy cuts both on each side's energy and on the sum of energy on both sides. This cut removes low energy clusters on both sides produced by the off-momentum particle accidental background.

The cluster energy distribution in DELPHI SAT is shown in Fig. 3 and compared to the Monte Carlo prediction with the BHLUMI⁵ generator. Only energy on the side which has lower energy is plotted. Data have a higher energy tail which is not seen in the Monte Carlo distribution. This tail is due to shower leakage in the diode readout of the calorimeter. The very small change of luminosity with the change of minimal energy cut is shown on a lower part of the plot. For DELPHI SAT it is very important to understand interactions on the mask edge since in this case only part of the shower energy is measured in the detector. Thus the energy cut effectively defines the geometrical acceptance of the detector. The Fig. 3 shows that the simulation of interactions on the mask edge is correctly described by the Monte Carlo.

3. Monte Carlo and experimental errors

Monte Carlo plays an important role for the luminosity measurements at LEP, as it does for the all LEP physics in general. There are two stages of the Monte Carlo generation. In the first one, the ideal physics event is generated by the "theorists' Monte Carlo", for example BHLUMI^{5,6} † However it does not give precisely the

*For $\mathcal{L}_{L,R}$ the fiducial acceptance cut is made only on one side, Left or Right.

†In this paper BHLUMI means the BHLUMI version 2. The version⁶ 4 is not yet (September 1994) used by LEP experiments.

OPAL SiW preliminary

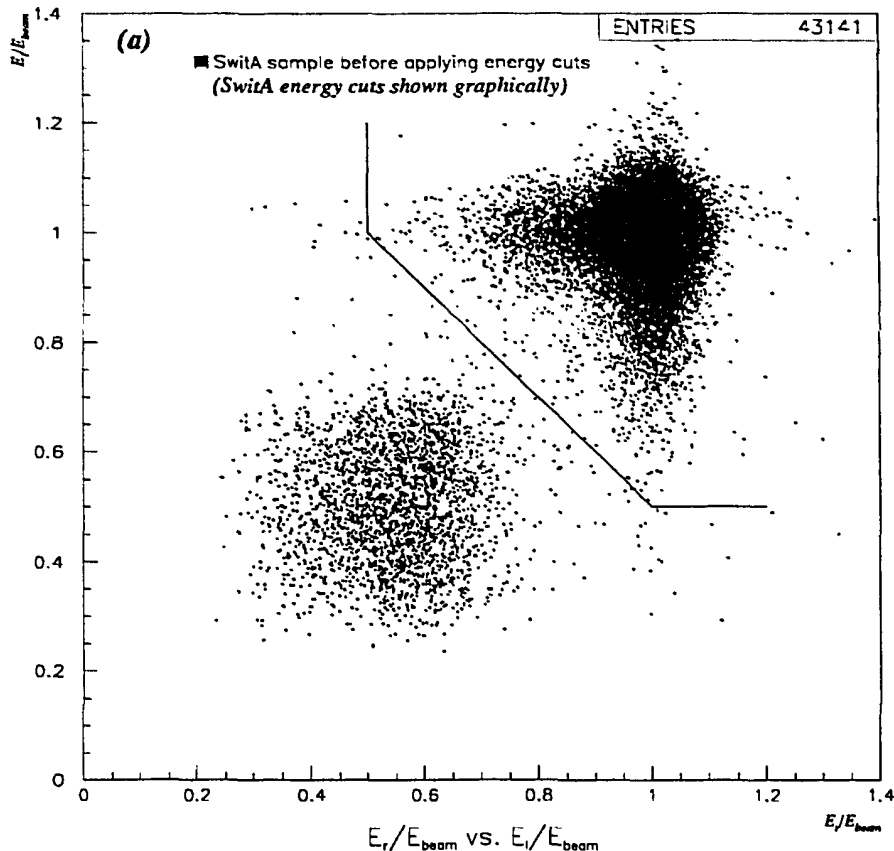


Figure 2: Energy measured on one side of the interaction point plotted against the energy measured on the other side in the OPAL second generation detector SiW. Energy cuts are shown as the solid line.

cross-section seen in the detector. We need to take into account a very complicated transformation of a "theorists' Monte Carlo" event by the detector and the detector environment. This is done in a second stage of the Monte Carlo generation in an "experimentalists' Monte Carlo". An event generated by BHLUMI is composed of a set of four vectors of electrons, positrons and photons. Interactions of these particles before the detector, for example in the beam pipe, need to be simulated. Particles can scatter there and interact producing additional particles. Then the detector response as exactly as possible, has also to be calculated for each particle. In this way we obtain events, seen as electronic signals in the detector, which look as close as possible to those produced by a "real" detector. These events pass then through the standard reconstruction program producing events composed of four vectors of particles. We can apply then the same cuts on the Monte Carlo events as

DELPHI SAT preliminary

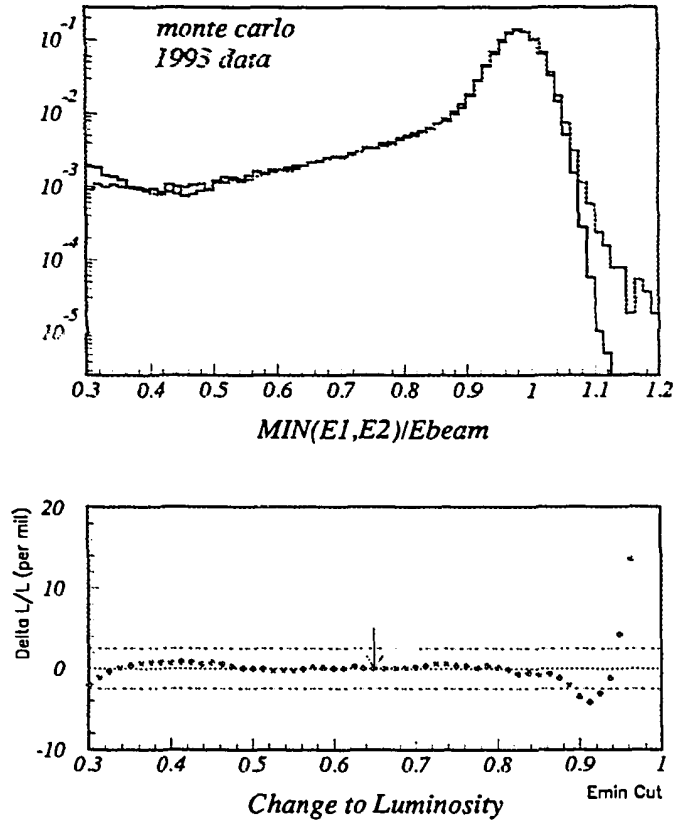


Figure 3: The cluster energy distribution on the side which has lower energy in the DELPHI SAT. The lower part of the plot shows the relative change of luminosity with the change of the minimal energy cut.

on the data. As a result we obtain the "Monte Carlo cross-section" used to calculate luminosity together with the measured number of events.

Events are selected by experimental cuts applied on the four vectors coming from the reconstruction program. Experimental errors appear if these cuts are not where we think they are, for example, a shift in Θ_{min} or Θ_{max} can have an important effect, as well as an experimental resolution, shifting events from below the cut to above and vice versa. The errors due to selection cuts are identified by the difference between the Monte Carlo simulation and data [‡] Since the result of the luminosity measurement should not depend on the variation of experimental cuts the size of errors is "measured" by varying these cuts as we could see on Fig. 3. Thus the experimental errors depending on the experimental selection can be reduced by the

[‡]In OPAL SiW pad curvature corrections are measured by comparing data taken with the muon and electron test beam.

improvement of both stages of the Monte Carlo simulation.

The second class of experimental errors are related to the precision of knowledge of the absolute position of the detector in space. These errors can only be reduced by a better geometrical survey of the detector; the improvements of the Monte Carlo simulation cannot reduce them.

4. Second generation LEP luminosity detectors

The basic parameters of the second generation LEP detectors are shown in the Table 2. Now the ALEPH, DELPHI and OPAL can place them closer to the beam line than the first generation detectors since the radius of the beam pipe has since been reduced to a diameter of 11 cm.

	R_{min} (cm)	R_{max} (cm)	Θ_{min} (mrad)	Θ_{max} (mrad)	app. xsection (nb)	technology
ALEPH SICAL	6.1	14.5	24	48	84	SiW
DELPHI STIC	7	18	31	185	65	lead+sc. tiles
L3 SLUM	7.6	15.4	29	58	50	BGO+silicon pl.
OPAL SiW	6.1	14.1	25	59	90	SiW

Table 2: Basic parameters of the second generation detectors at LEP.

L3⁷ has placed three planes of silicon in front of their BGO calorimeter (Fig. 4) on both sides in order to improve their luminosity measurement. BGO alone has limited granularity, the crystal size is 15 mm and also radius to Θ conversion is difficult. The silicon detector has a very sharp boundaries between strips: 1-2 μm , precise geometry known to better than 10 μm , fine granularity with 0.5 mm radial strips, and, since the detector is planar, easy radius to Θ conversion.

The data analysis is made in a following way: cluster coordinates are determined with the BGO and silicon strip hits are searched for in a small region around the BGO coordinates. If no hits are found, the BGO information is used. If one hit is found the silicon coordinate is used. If more than one hit is found the position of the silicon hits are averaged. The beam pipe geometry was modified on one side (Fig. 4) in order to limit the probability of electrons, positrons and photons to interact there, and for the majority of events only one silicon hit is observed. Since the beam pipe geometry was not modified on the other side about half of events have interactions on this side. These interactions have to be understood and well simulated by the Monte Carlo. Note that in a silicon plane only the electron(positron) and not photon hits are observed.

The DELPHI STIC⁸ is composed of lead and projective scintillator tiles of 3cm \times 22.5°. The light is collected by fibers. The cluster coordinates are measured by two silicon planes on each side with pad size of 1.3mm \times 22.5°. The acceptance on

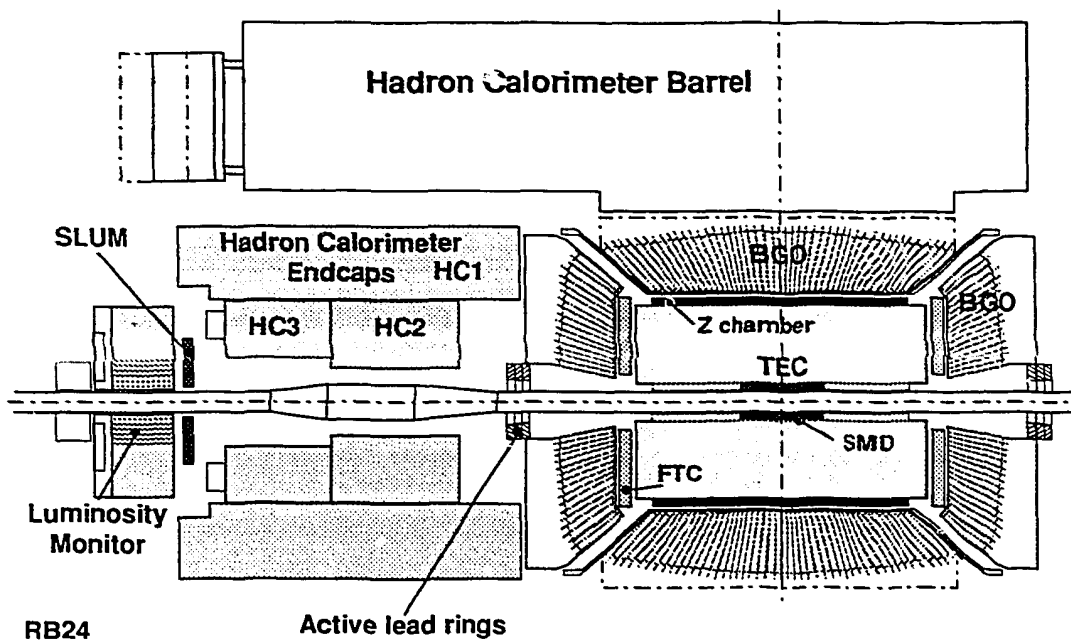


Figure 4: Three plans of silicon SLUM placed in front of the L3 BGO detector. Modification of beam pipe on one side is clearly seen.

one side is defined by a tungsten mask similarly as for the first generation detector. The STIC was installed in the beginning of 1994.

The ALEPH SICAL⁹ is composed of 12 two radiation length layers of tungsten. Use of tungsten as absorber allows the detector to be very compact, the total length is only 13 cm. The transverse dimensions of the shower are also very small. The Molière radius is 1cm in tungsten compared to 2.5 cm in lead and 2.4 cm in BGO. This improves the position resolution of the detector. The tungsten layers are sandwiched with the silicon planes with pad dimensions of $5.2\text{mm} \times 11.25^\circ$. The typical SICAL event is shown on Fig. 5. We can see there that the detector segmentation is sufficient for the observation of the transverse and longitudinal shower development. The cluster coordinates are measured by the silicon planes 3 and 4 placed in a region of maximum shower development. The R_{min} and R_{max} cuts are made on the pad boundary.

The OPAL SiW¹⁰ is similar to the ALEPH SICAL but the segmentation of the detector is more fine. The first 14 layers of tungsten have a thickness of one radiation length and they are followed by 4 layers of two radiation length. The radial pad size is half the size of the ALEPH SICAL one. The cluster coordinates are measured by 9 successive silicon planes starting from a layer number 3. This allows the precise measurement of the cluster Θ (or R) coordinates. The comparison of the measured

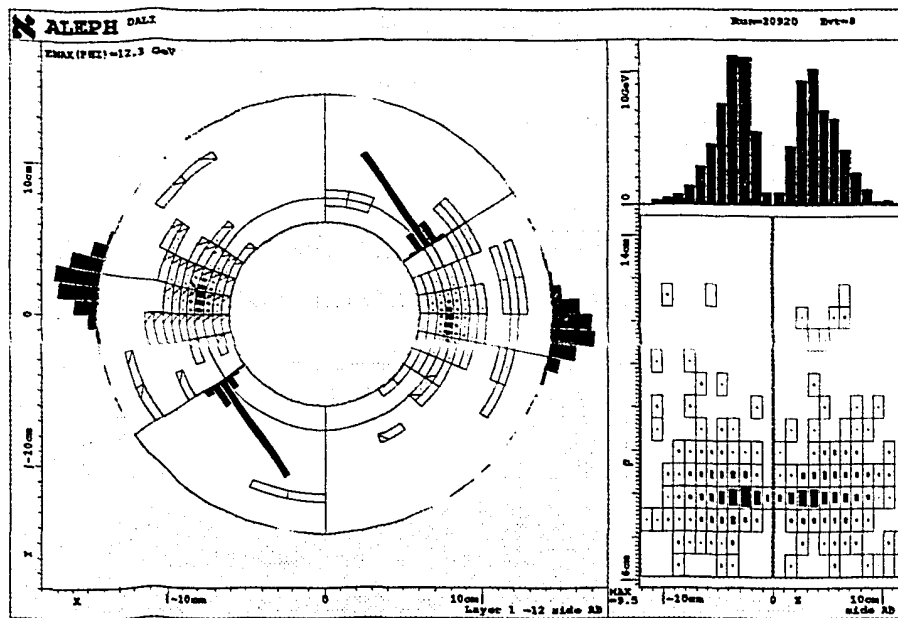


Figure 5: A typical event in the ALEPH SICAL detector. Two halves of the detector on two opposite sides containing electromagnetic shower are merged together into one picture. Transverse and longitudinal shower profiles are shown as black histograms.

R distribution with the one calculated with the help of Monte Carlo BHLUMI⁵ is shown on Fig. 6. The perfect agreement between these two distributions is observed. The R_{min} and R_{max} cuts are made on the pad boundary in the layer number 7. Having made this cut in any of four other neighboring layers changes the luminosity by less than a few parts in 10^{-4} .

A detailed list of the experimental errors contributing to the overall precision of the second generation detectors is presented in Table 3. All numbers are preliminary. ALEPH SICAL and L3 SLUM numbers were presented on the Moriond 94 Meeting while the OPAL SiW results were presented for the first time on the Glasgow 94 Conference. The purely experimental error of OPAL SiW is now already approaching the value of 6×10^{-4} . The ALEPH SICAL purely experimental error is 7.4×10^{-4} and will be improved in the future since, for example, the shower parametrization and simulation error in Table 3 was artificially inflated in the Moriond result to 0.036% from the value 0.023% for the 1992 results. So an ultimate precision of 5×10^{-4} is not excluded for these two detectors. The total experimental error is limited by the Monte Carlo statistics. If necessary this will be improved by a heavy use of computing time. L3 will also reduce its error in the future by the improvement of the energy cut as well as the z-separation measurement.

The precisions of the first and the second generation detectors are summarized in Table 4. A systematic improvement of the experimental precision with time was achieved by all experiments. These improvements were due to hardware upgrades.

OPAL SiW preliminary

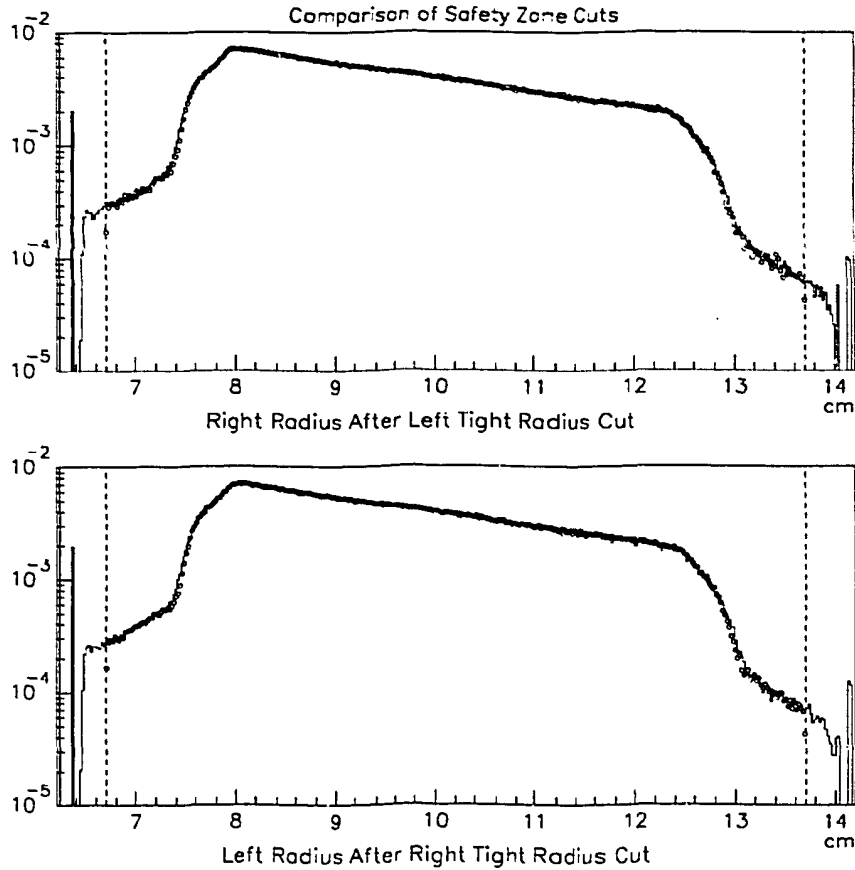


Figure 6: Radial distribution in the OPAL SiW detector compared to the Monte Carlo simulation with the BHLUMI generator.

due to better survey of the detector position as well as due to improvements of the detector simulation in the Monte Carlo. These improvements are well seen in the DELPHI SAT results where the lead mask was replaced by the tungsten mask, the geometrical survey was improved, and finally a lot of effort was put into the Monte Carlo simulation, particularly the simulation of interactions on the mask edge. Actual improvement with time was even bigger than what can be seen in Table 4 since some improvements, for example Monte Carlo simulation, could help in reducing the error of the data taken before the simulation was made.

	ALEPH SICAL	OPAL SiW	L3 SLUM	DELPHI STIC
Background estimation				
-Off momentum part.	0.003	0.001		
-Physics sources	0.010	0.001		i
Trigger efficiency	0.0002	< 0.0001	< 0.01	a n
Reconstruction efficiency	0.001			n
Radial fiducial cuts				a p
-Mechanical precision	0.029	0.036	0.033	l r
-Beam and mod. align.	0.030	0.02		y o
-z-separation	0.035	0.006	0.06	s g
-asymmetry or Θ cuts	0.026	0.026	0.034	i r
-shower param. and sim.	0.036	0.034		s c
-granularity (clustering)		0.01		s
-radial resolution		0.01		
Energy cuts	0.004		0.07	
Acoplanarity cut	0.005	0.01	0.02	
gap cut			0.02	
Subtotal experimental	0.074	0.062	0.12	
MC statistic	0.060	0.037	0.1	
Total experimental	0.095	0.072	0.16	< 0.2

Table 3: A detailed list of the experimental errors (in %) contributing to the precision of the second generation detectors at LEP and the total experimental error. All numbers are preliminary.

5. Use of the theoretical cross-section in the experiment

The basic Monte Carlo generator used by the LEP collaboration to generate e^+e^- scattering at small angles is BHLUMI⁵. It is a multiphoton generator with exclusive exponentiation of the Yennie-Frautschi-Suura type based on $O(\alpha)$ matrix element. It generates e^+e^- scattering through the t-channel photon exchange⁶ which represents 99% or more of the total e^+e^- cross-section. The second important component of the cross-section is the interference of the t-channel photon with the s-channel Z . In the Born approximation this contribution vanishes at the Z mass M_Z and can give up to 1% contribution at $M_Z \pm 1$ GeV for the first generation detectors. The interference of the s- and t-channel photons gives 0.15% contribution. Both of these interference contributions are included in BHLUMI in the Born approximation. However the $O(\alpha)$ corrections are very important for the photon- Z interference¹¹. They can reach 50% of the Born contribution above the M_Z . At the M_Z the $O(\alpha)$ correction is 0.2% for the first generation detectors¹¹. So the experiments remove the photon- Z part of the cross-section from BHLUMI (or

	1990	1991	1992	1993
ALEPH LCAL, SICAL	0.49	0.37	0.15	0.09
DELPHI SAT, STIC	0.8	0.5	0.38	0.28
L3 BGO, SLUM	0.5	0.5	0.5	0.16
OPAL FD, SiW	0.7	0.45	0.41	0.07

Table 4: Precision (in%) of the luminosity detectors at LEP for different periods of data taking. Names and precision of the second generation detectors are marked in bold. ALEPH SICAL was operational since September 1992. The 1992 precision of LCAL was 0.37%. The DELPHI STIC is operational since the beginning of 1994.

run BHLUMI at the Z mass) and correct the BHLUMI cross-section by the $O(\alpha)$ photon- Z cross-section calculated with the help of the BABAMC¹² (or BIHAGEN¹³ for OPAL) Monte Carlo generator. It has been shown¹¹ that the BABAMC $O(\alpha)$ calculation of the Z -exchange terms have a technical precision of 3×10^{-4} . For the second generation detectors, the photon- Z contribution is about 4 times smaller[§]. The error of this contribution is related to the higher order corrections missing in the calculation. Thus this error is about four times smaller for the second generation detectors. The summary of the different contributions to the total theoretical error¹¹ are presented in Table 5. Note also that the vacuum polarization error is smaller for the second generation detectors. This error is related to the hadronic vacuum polarization component calculated by the dispersion relations from the low energy e^+e^- annihilation into hadrons. Main reason for this change is that the vacuum polarization part of the total cross-section is reduced to about 4% from more than 5% for the first generation detectors¹¹. The largest contribution to the theoretical error, the BHLUMI error, should be reduced in the near future⁶. The semianalytical calculations of the small angle bhabha scattering with the precision of 10^{-3} are in progress¹⁴. The e^+e^- scattering into photons has contribution of about 2×10^{-4} for the acceptance of the second generation detectors. The other sources of the physics background are small⁹.

6. Relative luminosity measurement and calculations

Up to now we have discussed the absolute error of the luminosity measurement and calculations. This error is important for the σ_0 measurement, as was mentioned in the Introduction. For the M_Z and Γ_Z measurements only the center-of-mass dependent relative luminosity errors contribute.

The relative luminosity errors are much smaller than the absolute ones since the absolute detector position and absolute value of the event selection cuts do not contribute and only their relative change from one energy point to the other one has to be taken into account. Special care has to be given to the LEP beam

[§]L3 had a smaller photon- Z contribution already for the first generation detector.

Contribution	$3.3^\circ - 6.3^\circ$	$1.61^\circ - 2.8^\circ$
(1) $O(\alpha^2)$ LL BHLUMI	0.15	0.15
(2) $O(\alpha^2)$ SL BHLUMI	0.09	0.09
(3) Z exchange $O(\alpha)$ BABAMC	0.03	0.03
(4) Z exchange $O(\alpha^2)$ LL BABAMC	0.06	0.015
(5) Z exchange $O(\alpha^2)$ SL BABAMC	0.06	0.015
(6) Vacuum polarization	0.08	0.05
Total theoretical error	0.28	0.25

Table 5: Summary of theoretical errors on the luminosity calculation in different angular regions¹¹. The first angular region represents a typical acceptance of the first generation detectors while the second one corresponds to the acceptance of the second generation detectors.

movements. The interaction vertex position can vary from fill to fill and even some correlation may exist between the center-of-mass energy and the vertex position. The luminosity measurements are independent of the vertex position movement in the first order but the second order gives typically the largest component of the relative error. This can be observed in the Table 6. We see there that the relative experimental luminosity errors of the second generation LEP detectors are in the 2×10^{-4} range. For ALEPH this is true for the subtotal experimental error. The total experimental error is limited by the Monte Carlo statistics. Since this is statistics of the Monte Carlo generator without detector simulation it can be reduced to a negligible level with a little use of computer time.

The relative luminosity error of the L3 SLUM is considered to give a negligible contribution to the M_Z and Γ_Z measurement¹⁵ with the 1993 LEP energy scan¹⁶, however a detailed error analysis has not yet been officially given.

The LEP experiments have another set of luminosity counters placed at a very small angle. They are placed after superconducting quadrupoles of the LEP focusing system. These quadrupoles are focusing in one plane and defocusing in the other one so these counters have access to very small angles of a few milliradians. Their high counting rate allows approximate instantaneous luminosity measurement during data taking and beam adjustment. They are however not generally used by LEP experiments in physics analysis. DELPHI has made a special effort to use these counters for their relative luminosity measurement. The DELPHI VSAT¹⁷ is composed of four small silicon-tungsten calorimeters placed symmetrically around the beam pipe after the low β quadrupoles at ± 7.7 m from the interaction point. It covers polar angles of 5-7 mrad and its cross-section is about 18 times the Z hadronic one. However its acceptance is very complicated. It depends on the beam position, divergences, width and tilt, on the quadrupole focusing and defocusing depending on its current, and on the interactions of particles before the detector. All these have been studied with the Monte Carlo simulation and corrections to the observed

	ALEPH SICAL	OPAL SiW
Beam related systematics	0.021	0.005
Energy scale and resolution	0.006	0.005
Θ cut	0.008	0.010
cluster finding efficiency		0.002
backgrounds		0.01
no detector simulation	0.006	
subtotal experimental error	0.024	0.02
MC statistics	0.061	
total experimental relative error	0.066	0.02
total theoretical relative error	0.02	0.02

Table 6: A detailed list of the experimental errors (in %) contributing to the center-of-mass dependent relative precision of the ALEPH SICAL and OPAL SiW and the total relative experimental error. All numbers are preliminary and have been used for the preliminary analysis presented on the Moriond 94 meeting. Relative precision of the DELPHI VSAT and L3 SLUM are described in the text.

cross-section have been introduced for each data set recorded on the cassette. The relative systematic error is of the order of 10^{-3} or better. This method has an advantage of a strong reduction of the statistical error of the relative luminosity measurements since the VSAT cross-section is about 500 nb.

The relative luminosity theoretical errors have been already discussed¹⁸. The BHLUMI errors as well as the vacuum polarization error shown in Table 5 cancel for the relative luminosity measurement and only the $C(\alpha^2)$ Z exchange terms have to be taken into account. The conclusion is¹⁸ that these errors do not reduce the precision of the M_Z and Γ_Z measurement made during the 1993 LEP energy scan¹⁶ for the second generation luminosity detectors located at small angles. However in case of a possible future energy scan the influence of the relative theoretical errors should be reanalysed.

The results presented in this talk have been obtained by four LEP experiments. I would like to thank B. Bloch, A. Blondel, G. M. Dallavalle, S. Jadach, M. Koratzinos, E. Laucon, M. Mannelli, E. Martin, M. Merk, D. Miller, R. Miquel, J. Rander and T. Todorov for their help in preparation of this talk and B.F.L. Ward for excellent organization of this meeting. Part of this work has been done in a framework of the Cracovie-LAPP IN2P3 Collaboration.

REFERENCES

1. D.Decamp et al., Z.Phys. C53(1992)375.
2. P. Abreu et al., preprint CERN-PPE/94-08:CERN/94-31; DELPHI internal note DELPHI 94-9 PHYS 354.
3. OPAL internal note OPAL TN-128; R. Akers et al., Z.Phys. C60(1993)601.
4. O. Adriani et al., Phys. Reports 236(1993)1.
5. S. Jadach, E.Richter-Was, Z. Was and B.F.L. Ward, Phys.Lett. B268(1991)253; Comput. Phys. Commun. 70(1992)305.
6. S. Jadach et al., this proceedings.
7. M. Merk, to appear in the Proc. of the XXIXth Rencontres de Moriond, Electroweak Int. and Unified Theories, Méribel, March,1991, Ed. J. Trân Thanh Vân.
8. LEPC document CERN/LEPC/92-6;LEPC/P2-Add.1.
9. D. Buskulic et al.,Z.Phys. C62(1994)539, B. Bloch-Devaux et al., ALEPH internal note ALEPH 93-149, PHYSICS 93-129.
10. LEPC document CERN/LEPC91-8.LEPC/M-100; OPAL internal note OPAL TN-221;PN-142; J. Hart, to appear in the Proc. of the Rencontres de Physique de la Vallee D'Aoste, La Thuile, March 1994.
11. W. Beenakker and B. Pietrzyk, Phys. Lett B296(1992)241; B304(1993)366.
12. M. Böhm, A. Denner and W.Hollik, Nucl. Phys. B304(1988)687; F.A. Berreids, R. Kleiss and W. Hollik, Nucl. Phys. B304(1988)687.
13. M. Caffo, H. Czyz and E. Remiddi, Il Nuovo Cimento 105A(1992)277.
14. E. Kuraev et al., this proceedings.
15. The L3 Luminosity Group, private communication.
16. A. Blondel, this proceedings.
17. DELPHI internal note DELPHI 92-77 PHYS 188.
18. M. Martinez and B. Pietrzyk, Phys. Lett. B324(1994)497